Check for updates

JOURNAL OF
biomaterials
applications

Biomaterials Processing

Journal of Biomaterials Applications
2025, Vol. 39(6) 592–606
© The Author(s) 2024

Article reuse guidelines:
sagepub.com/journals-permissions
DOI: 10.1177/08853282241268673
journals.sagepub.com/home/jba
Sage

Boric acid and zinc borate doped graphene hydrogels designed for burn treatment: In vitro viability-biocompatibility tests and microbiological analysis

Yasin Bayir[1], Beyzagül Erkayman[2], Abdulmecit Albayrak[3], Şaziye Sezin Palabiyik-Yücelik[4], Sümeyra Can[5], Hayrunisa Hanci[6], Fatih Tunç[1], Hamza Halici[3], Maide Sena Civelek[3], Melike Sevim[5], Emir Enis Yurdgülü[1] and Önder Metin[7]

Abstract

Boron, an essential element for human, can be a key factor in wound healing. For this reason, in this study, role of boron products (boric acid and zinc borate) and boron product doped new synthesized graphene hydrogels was investigated for burn healing via in vitro viability-biocompatibility tests and microbiological analysis. It has been determined that boric acid and zinc borate are effective against microbial agents that are frequently seen in burns. In L929 mouse fibroblast cell line, BA, ZB and graphene hydrogels did not show any toxic effects, either alone or doped Graphene Hydrogel forms, except at very high doses. These substances showed antioxidant properties by protecting cells against H_2O_2 damage. The migration test performed on boron products also confirms the protective effect of boron products. In this study, the synthesis of graphene hydrogels was made for the first time, and their characterization was completed with appropriate instrumental analyses. The results of the biocompatibility tests of graphene hydrogels show that they are at least 96% biocompatible.

Keywords

Boric acid, zinc borate, graphene hydrogels, viability, biocompatibility, microbiological analysis

Introduction

Boron, whose main sources are diet and drinking water, is an essential element for humans.[1] Boron is absorbed nearly 100% by the digestive and respiratory systems and is distributed to all tissues as boric acid.[2] Since boron, which is eliminated by the body, cannot accumulate in the body, it may be necessary to take supplements from outside. Boron deficiency affects various metabolic events in the body, causing decreased immune function and a high risk of osteoporosis.[3] For this reason, Boron is a very important substance in embryogenic development, regulation of bone metabolism, functioning of antioxidant mechanisms and wound healing.

Wound healing is a physiological process that develops in response to injuries.[4] This process consists of sequential phases of hemostasis/inflammatory, proliferative and remodeling.[5] After tissue injury, the coagulation cascade and inflammatory cell accumulation begin and cytokines are produced in the tissue.[6,7] Inflammatory cells such as macrophages and mast cells trigger fibroblast migration into tissue.[8] Activated fibroblasts and keratinocytes provide tissue integrity via reducing wound size. The effective role of

[1]Department of Biochemistry, Faculty of Pharmacy, Ataturk University, Erzurum, Türkiye
[2]Department of Pharmacology, Faculty of Pharmacy, Ataturk University, Erzurum, Türkiye
[3]Department of Pharmacology, Faculty of Medicine, Ataturk University, Erzurum, Türkiye
[4]Department of Pharmaceutical Toxicology, Faculty of Pharmacy, Ataturk University, Erzurum, Türkiye
[5]Department of Chemistry, Faculty of Science, Ataturk University, Erzurum, Türkiye
[6]Department of Microbiology, Faculty of Pharmacy, Ataturk University, Erzurum, Türkiye
[7]Department of Chemistry, College of Sciences, Koc University, İstanbul, Türkiye

Corresponding author:
Yasin Bayir, Department of Biochemistry, Faculty of Pharmacy, Ataturk University, Erzurum 25240, Türkiye.
Email: yasinbayir@hotmail.com

fibroblasts in wound healing has been the target of many in vitro and in vivo models. Experiments on skin fibroblast cell line are the most preferred ones.[9] Many fibroblasts that mimics wound healing process are cultured. L929 (mouse fibroblast) cell line is the most used cell line among cell lines.

Boron compounds produced from boron have been used in a wide variety of fields besides the health field. There are many boron components such as boric acid, para-borophenylalanine, diazoborine, boronic acid, sodium borate, zinc borate.[10] It has been reported that boric acid is used in the treatment of burns in clinics. In a study, it was reported that the effect of Boric acid on wound healing is probably by increasing EphrinB1, EphrinB2 and EphB4 and decreasing increased TNF-α levels.[11] Sodium borate and boric acid salt, one of the boron derivatives, has been reported to increase cell migration in human keratinocyte cells without affecting proliferation.[12] Sodium borate has been shown to provide tube-like structural formation in cell culture and increase vascularization in wound healing in vitro.[13] In addition, boron doped new materials can be shown to make better human health in the literature.[14]

Zinc is a very important substance that increases wound healing routinely used in the clinic.[15] Zinc, an essential micronutrient for humans; important in the regulation of lipid, protein and nucleic acid metabolism and gene transcription.[16] Topical zinc oxide is also used in the treatment of atopic dermatitis due to its antioxidant and antibacterial effects. In addition, zinc oxide also increases collagen degradation in necrotic tissues. One of the newly synthesized boron compounds containing the zinc compound is zinc borate. Zinc borate is formed by special reaction series of Zinc and boric acid.

Graphene hydrogels formed by 3D carbon networks are porous materials that hold 95%–99% water molecules in their pores. On the other hand, the graphene aerogels, the structural analogous of graphene hydrogels, are the porous materials where the pores are filled with air. In this respect, graphene hydrogels can be thought as the water filled graphene aerogels. Graphene hydrogels provide a moist environment at the wound and dressing interface, performs air/gas exchange, prevents the entry of microorganisms from the outside, and most importantly, accelerates healing by removing body fluids in wound healing.[17] In addition, it is known that hydrogels are used in a wide spectrum from drug release to biomedical applications due to their advantageous properties such as non-adhesion to the wound surface, pain relieving properties and reducing wound temperature. Biocompatible graphene can be economically synthesized on a large scale by chemical delamination and subsequent reduction of graphene oxide (GO).[18,19] Thanks to their 3D carbon network and porous structures, graphene hydrogels possess a large water holding capacity, high biocompatibility, non-toxicity, excellent thermal and electrical conductivity compared to other hydrogels.[20]

The aim of this research is to investigate the role of two boron compounds (boric acid and zinc borate); in both pristine and graphene hydrogel-doped forms; in cell viability test in the L929 mouse fibroblast cell line and their antioxidant effect against hydrogen peroxide damage. In addition, antibacterial effect and wound healing potential of boric acid and zinc borate compounds were studied. Irritation potential and biocompatibility of pristine and boron compound doped graphene hydrogels on the skin were also determined by the In Vitro EpiDerm Skin Irritation Test.

Methods

Boron products experiments

Chemicals. Boric Acid and Zinc borate which obtained from Eti Mining Operations General Directorate (ETİMADEN), Turkiye was selected and used in different concentrations during studies.

Antimicrobial activity of boron products. The antimicrobial activities of boron products were determined with 11 different microorganisms (*Staphylococcus aureus* ATCC 29213, *Enterococcus faecalis* ATCC 29212, *Streptococcus pyogenes* ATCC 19615, *Escherichia coli* ATCC 25922, *Klebsiella pneumoniae* ATCC 700603, *Pseudomonas aeruginosa* ATCC 9027, *Acinetobacter baumannii* ATCC 19606, *Proteus mirabilis* ATCC 25933, *Candida albicans* ATCC 10231, *Aspergillus niger* ATCC 16888 standard microorganism strains and a clinical isolate *Serratia mercescens*).

Broth macrodilution method was used to determine the antimicrobial susceptibility (*minimum inhibitory concentrations (MIC)*) of the strains. In this method, 10 tubes were prepared for each microorganism and two-fold serial dilution of boron products were made starting from the first tube to the last tube (the highest concentration was determined as 3% for boric acid and 9% for zinc borate). Dilution tests were performed in accordance with CLSI recommendations. Cationized Mueller Hinton Broth (CMHB) medium was used for bacterial strains and RPMI 1640 medium was used for fungal strains.[21,22] *For the Determination of minimum bactericidal concentrations (MBC),* from all tubes without growth in the macrodilution test, cultures was performed on solid media and the lowest concentration without microorganism growth was determined.

Cytotoxicity of boron products. The proliferative effects of boric acid (6 concentrations) and zinc borate (6 concentrations) on the L929 (mouse fibroblast) cell line at 24, 48 and 72 h were investigated. The L929 cell line from the American Type Culture Collection (ATCC, USA) in Cryotube was removed from the liquid nitrogen tank and added to the T75 cm^2 humanized DMEM flask containing 10% FBS and incubated in 37°C and 5% CO_2 oven.

Cells were passaged sequentially, and after the fourth passage, cell counts were made and 5000 cells were seeded into each well of the 96-well plate. The cells were incubated in a CO_2 oven for 24 h to settle at the bottom of the well. At the end of this time, the relevant doses of boron products (for boric acide 0.001 mM - 1000 mM, for zinc borate 0.001 mM - 1 mM) were administrated into whells. For 24^{th}, 48^{th}, 72^{nd} hours, measurements were made with the MTT method with a microplate reader spectrophotometer (Epoch Microplate Spectrophotometer, BioTek, USA) at an absorbance value of 570 nm. Viability rates were analyzed by comparison with control wells.

Antioxidant Ability of boron products. In order to determine the protective effects of boric acid and zinc borate against the oxidative stress caused by H_2O_2 in the cell, L929 cells were repassed and were challenged by different (0.3, 0.4, 0.5, 0.6, 0.7, 0, 8, 0.9 mM) H_2O_2 concentrations. For this reason, the effects of 0.001 mM - 1000 mM for boric acid and 0.001 mM - 1 mM for zinc borate concentrations on L929 cells were investigated by MTT method. Inoculation was done in a 96-well plate. Twenty-4 hours later, cells were exposed to different concentrations of boric acid and zinc borate, and 3 hours later, H_2O_2 (selected-0.4 mM) was added to the medium. Afterwards, at 24^{th}, 48^{th}, 72^{nd} hours, the cells were measured with an absorbance value of 570 nm with a microplate reader spectrophotometer (Epoch Microplate Spectrophotometer, BioTek, USA) using the MTT method. Viability rates were analyzed by comparison with control wells.

Cell migration of boron products. The L929 cell line obtained from the American Type Culture Collection (ATCC, USA) and located in the Cryotube was removed from the liquid nitrogen tank and inoculated into a T75 cm^2 flask containing DMEM medium with 10% FBS and incubated at 37°C, 5% CO_2 oven. After the fourth passage, cells were counted and inoculated into 24 well plates at 2×10^5 cells/ml. The cells were incubated in a CO_2 oven for 24 h to settle on the bottom of the plate. After observing that the cells formed an entire layer at the bottom of the well, the cells were lifted from the bottom by creating a vertical scratch in each well with a sterile pipette tip. Images were taken on the first day (day 0) using a Leica Inverted Microscope (Leica, DMIL LED). Immediately after the images were recorded, drug cultivation was performed and the images were taken again with the Leica Inverted Microscope (Leica, DMIL LED) at the 12^{th} and 24^{th} hours (10x).

Boric acid and zinc borate doped graphene hydrogel products experiment

Instrumental analysis methods. The chemicals used for the synthesis of graphene aerogels (P_2O_5, $KMnO_4$, $NaNO_3$, H_2SO_4, natural graphite flakes (325 mesh), H_2O_2) were purchased from Alfa Aesar®.

Structural characterization of the synthesized materials was carried out by using many advanced analytical methods. Transmission electron microscopy (TEM) images were conducted on a Hitachi HighTech HT7700 (120 kV) working at high-resolution (HR) mode. PANalytical Empyrean diffractometer (Cu K alfa radiation, 1.54 Å) was used to record XRD patterns. X-ray photoelectron spectroscopy (XPS) measurements were conducted on a Specs-Flex X-ray photoelectron spectrometer with an aluminum anode (Al Kα, 1468.3 eV). Scanning electron microscopy (SEM) images were recorded on a Zeiss Sigma 300 Field Emission Scanning Electron Microscope. The elemental analysis were performed by Agilent 7800 inductive-coupled plasma mass spectroscopy (ICP-MS). The graphene hydrogels were dried by using a CHRIST Alpha 1-4 Ldplus lyophilizer.

Synthesis of graphene aerogels. Graphene aerogels were synthesized by using a 3-step method starting from natural graphite flakes. Graphene oxide was synthesized by using well-established modified Hummers method available in the literature.[23]

Graphene hydrogel synthesis using graphene oxide. A homogeneous graphene oxide solution was prepared by dissolving 0.2 g of graphite oxide in 80 mL of distilled water with the help of sonication. The resulting solution was placed in a Teflon-coated stainless steel hydrothermal reactor and heated in an oven at 180°C for 18 h. At the end of the process, initial bright yellow color of graphene oxide solution was disappeared and black cylindrical structures were obtained, indicating the formation of graphene hydrogels. Next, as-synthesized graphene hydrogels were frozen at −80°C overnight and made ready for vacuuming in a lyophilizer device to turn them into graphene aerogels. Graphene aerogels were prepared by drying overnight (12 h) in a vacuum environment of 0.630 mbar in a lyophilizer device.

Loading of graphene aerogels with different doses of boric acid and zinc borate. To load the boric acid into the graphene aerogel structure, aqueous solution of 1.5 wt% and 3 wt% boric acid were prepared by dissolving 150 mg and 300 mg of boric acid in 10 mL of distilled water. Next, as-prepared dry graphene aerogels were added into the boric acid solutions and the mixture was allowed to stir for a while to ensure the soaking up of boric acid solution by graphene aerogels. Then, excess solution was removed, and the resultant wet powder materials were dried in an oven at 80°C.

In the case of zinc borate loading to graphene aerogels, aqueous solutions containing 4.5 wt% and 9 wt% zinc

borates were prepared by dissolving 450 and 900 mg of zinc borate in 10 mL of distilled water, respectivel. Since zinc borate is not very soluble in water, a trace amount of weak acid (acetic acid) was added to the zinc borate solutions to ensure the dissolution of all zin borates. After dissolving the zinc borate, the dry graphene aerogels were added to the zinc borate solutions and the mixture was allowed to stir for a while to ensure the soaking up of boric acid solution by graphene aerogels. Then, excess solution was removed, and the resultant wet powder materials were dried in an oven at 80°C.

Water retention and swelling. The swelling test, which is widely used in the literature, was applied to determine the water holding capacity of the synthesized graphene aerogel materials.[2] The obtained graphene aerogels were immersed in containing zinc borate and boric acid aqueous solutions at room temperature. The swelling ratios were calculated by the following equations:

$$\text{Swelling ratio}\,(\%) = (W_t - W_0)/W_0 \times 100 \qquad (1)$$

Where W_t (g) and W_0 (g) represent the weights of the dry sample and swollen sample, respectively. While the swelling capacity of graphene aerogel for a solution containing 1.5% boric acid was 2250, the swelling capacity of graphene aerogel for a solution containing 3% boric acid was calculated as 1311. However, the swelling capacities of the solutions containing 4.5% and 9% zinc borate were calculated as 963 and 831, respectively. As the amount of material taken into the graphene aerogel increases, the swelling capacity decreases.

Biological characterization of boric acid and zinc borate doped graphene hydrogels. Cell Culture and Cytotoxicity and Antioxidant Ability of Boric Acid and Zinc borate doped Graphene Hydrogel were performed like in only boron products methods. In cell culture and oxidative stress experiments doses we used were 0.2%–0.013% for graphene hydrogel, 3% - 0.094% for boric acid doped graphene hydrogel and 9% - 0.28% for zinc borate doped graphene hydrogel.

In Vitro EpiDermTM skin irritation test for boric acid and zinc borate doped graphene hydrogels. In Vitro EpiDerm™ Skin Irritation Test (EpiDerm SIT) (MatTek, Ashland, USA) were performed to evaluate the skin irritation potential and biocompability of the graphene hydrogels. Safety evaluation of the graphene hydrogels were assessed with this test. The cytotoxic effect of graphene hydrogels on 3D human epidermis model consists of normal human-derived epidermal keratinocytes was determined according to the OECD 439 guideline.[24] This test is also ECVAM validated alternative test for the traditional animal skin irritation test and based on application on a 3D human epidermis model consists of normal human-derived epidermal keratinocytes and measurement of cell viability by MTT test [3-(4,5-dimethylthiazol-2-yl)-2,5-diphenyl-tetrazolium bromide colorimetric test]. Dulbeccos's phosphate-buffered salin (DPBS) used as a negative control and sodium dodecyl sulfate (SDS) used as positive control in this assay. The graphene hydrogel samples were made ready for use by adding 1 mL of distilled water to 50 mg sample. In this study, the effect of the tested substances on cell viability was measured quantitatively with the MTT method simultaneously with the negative and positive control. The alteration of cell viability of the tissues exposed to graphene hydrogels in comparison to NC were shown the skin irritation potential of the materials. The relative cell viability over 50% was accepted as "non-irritant substance" according to EpiDerm SIT protocol and assessed by using the given formula below[25]:

$$\textit{Relative viability of test sample}\,(\%) = \left[OD_{TS}/\textit{Mean of } OD_{NC}\right] \text{x} 100 \qquad (2)$$

OD_{TS} is the OD of the test sample (TS) and OD_{NC} is the OD of NC

Results and discussion

Results were given below as of two boron compounds (boric acid and zinc borate); in both pristine and graphene hydrogel-doped forms; in cell viability test in the L929 mouse fibroblast cell line and their antioxidant effect against hydrogen peroxide damage. Additionally, antibacterial effect and wound healing results of boric acid and zinc borate compounds and Irritation potential and biocompatibility of pristine and boron compound doped graphene hydrogels on the skin results were also presented.

Boron products experiments

Antimicrobial analyses of boron products. In the macrodilution test, it was observed that boric acid and zinc borate were effective on all microorganisms in general, and had inhibitory effects especially on *S. pyogenes* ATCC 19615 and *C. albicans* ATCC 10231 and *A. niger* ATCC 16888 even at very low concentrations. However, it was observed that MIC and MBC values in Gram-negative bacteria were high. Boric acid had no bactericidal effect on *E. faecalis, K. pneumoniae, P. aeruginosa, A. baumannii* and zinc

borate had no bactericidal effect on *E. faecalis, P. mirabilis, S. mercescens*, *A. niger* strains. The MIC and MBC values of boric acid and zinc borate for each microorganism as a result of the macrodilution test are given in Table 1. According to the results of the tests carried out to determine the effectiveness of the hydrogels, it was determined that the hydrogels impregnated with boric acid and zinc borate did not have a reducing effect on the number of bacteria.

Our results of the macrodilution study showed that boric acid and zinc borate were effective in inhibiting the growth of microorganisms even below the determined concentrations. In the literature, it is seen that the antimicrobial activity of boric acid has been reported at varying rates.[26,27] Moreover, it has been understood that our study is quite rich in terms of microorganism diversity used in the evaluation of antimicrobial susceptibility. Although this situation limits us in terms of comparing our results, it is a positive factor in terms of contributing to the literature for future studies.

Cytotoxicity analyses of boron products. The proliferative effects of varying concentrations of boric acid (0.001 mM-1000 mM) and zinc borate (0.001 mM-1 mM) on the L929 (mouse fibroblast) cell line at 24, 48, and 72 h are shown in Figure 1. When the effect of boric acid on L929 mouse fibroblast cells, which were divided into six groups in which 0.001 mM and 1000 mM concentrations were applied, at 24th, 48th and 72nd hours compared to the control group, no significant proliferation or inhibition was observed in the cells at any concentration except 100 mM and 500 mM for 24th hour, 100 mM for 48th hour (Figure 1(A)). In general, insignificant IC50 values and insignificant differences between concentrations showed no negative viability effect on 24th hour on L929 cells. In literature, it was found that boric acid did not show an inhibitory effect on different cell lines in in vitro conditions and showed wavy U-shaped results, similar to our study.[28,29] In addition, studies have reported that the effect of boric acid on growth is dependent on cell type.[30,31] The use of boric acid in wound healing in the clinic and the absence of any toxic effects support our results.[32,33] We think that the reason for this non-toxic and non-proliferating effect at very high doses, at a concentration of 1000 mM, may be that boric acid does not enter the cell.

When the effects of zinc borate on L929 mouse fibroblast cells of six groups between 1 mM and 0.001 mM concentrations were compared with the control group at 24^{th}, 48^{th} and 72^{nd} hours, a statistical difference was observed in terms of proliferative or inhibitory effect in all concentrations (Figure 1(B)). Inhibitor concentration IC50 dose that caused 50% decrease in cell proliferation at 24^{th} hour was 0.133 mM, IC50 dose at 48^{th} hour was 0.197 mM, and IC50 dose at 72^{nd} hour was 0.142 mM. These results show that zinc borate has an inhibitory effect on L929 mouse fibroblast cells from 1 mM to 0.133 nm, and a prophylactic effect at lower concentrations at 24^{th} hours. Zinc borate has an inversely proportional effect on L929 mouse fibroblast cells at 48^{th} and 72^{nd} hours.

Considering that boric acid does not affect L929 cell proliferation positively or negatively, we can think that the inhibitory or proliferative effect of zinc borate is due to zinc. We hypothesize that zinc decreases cell viability up to a certain concentration and increases cell viability beyond this threshold. Çelikezen et al. proved that in a different cell type zinc borate has antioxidant properties of at low

Table 1. The MIC and MBC values of boric acid and zinc borate.

	Boric acid (3%)		Zinc borate (9%)	
Microorganism	MIC (%)	MBC (%)	MIC (%)	MBC (%)
S. aureus ATCC 29213	0.75	0.75	0.125	4.5
E. faecalis ATCC 29212	1.5	>3	0.0351	>9
S. pyogenes ATCC 19615	0.0058	3	0.0175	0.2812
E. coli ATCC 25922	0.375	1.5	0.0351	0.5625
K. pneumoniae ATCC 700603	0.75	>3	0.1406	2.25
P. aeruginosa ATCC 9027	0.75	>3	4.5	1.125
A. baumannii ATCC 19606	0.375	>3	1.125	9
P. mirabilis ATCC 25933	0.75	3	4.5	>9
S. mercescens	0.375	3	4.5	>9
C. albicans ATCC 10231	0.0058	0.0058	0.0175	0.0175
A.niger ATCC 16888	0.0058	0.1875	0.0175	>9

Boric acid and zinc borate are effective against microbial agents that are frequently seen in burns. In L929 mouse fibroblast cell line, BA, ZB and graphene hydrogels did not show any toxic effects, either alone or doped Graphene Hydrogel forms, except at very high doses. These substances showed antioxidant properties by protecting cells against H_2O_2 damage. The migration test performed on boron products also confirms the protective effect of boron products. In this study, the synthesis of graphene hydrogels was made for the first time, and their characterization was completed with appropriate instrumental analyses. The results of the biocompatibility tests of graphene hydrogels show that they are at least 96% biocompatible.

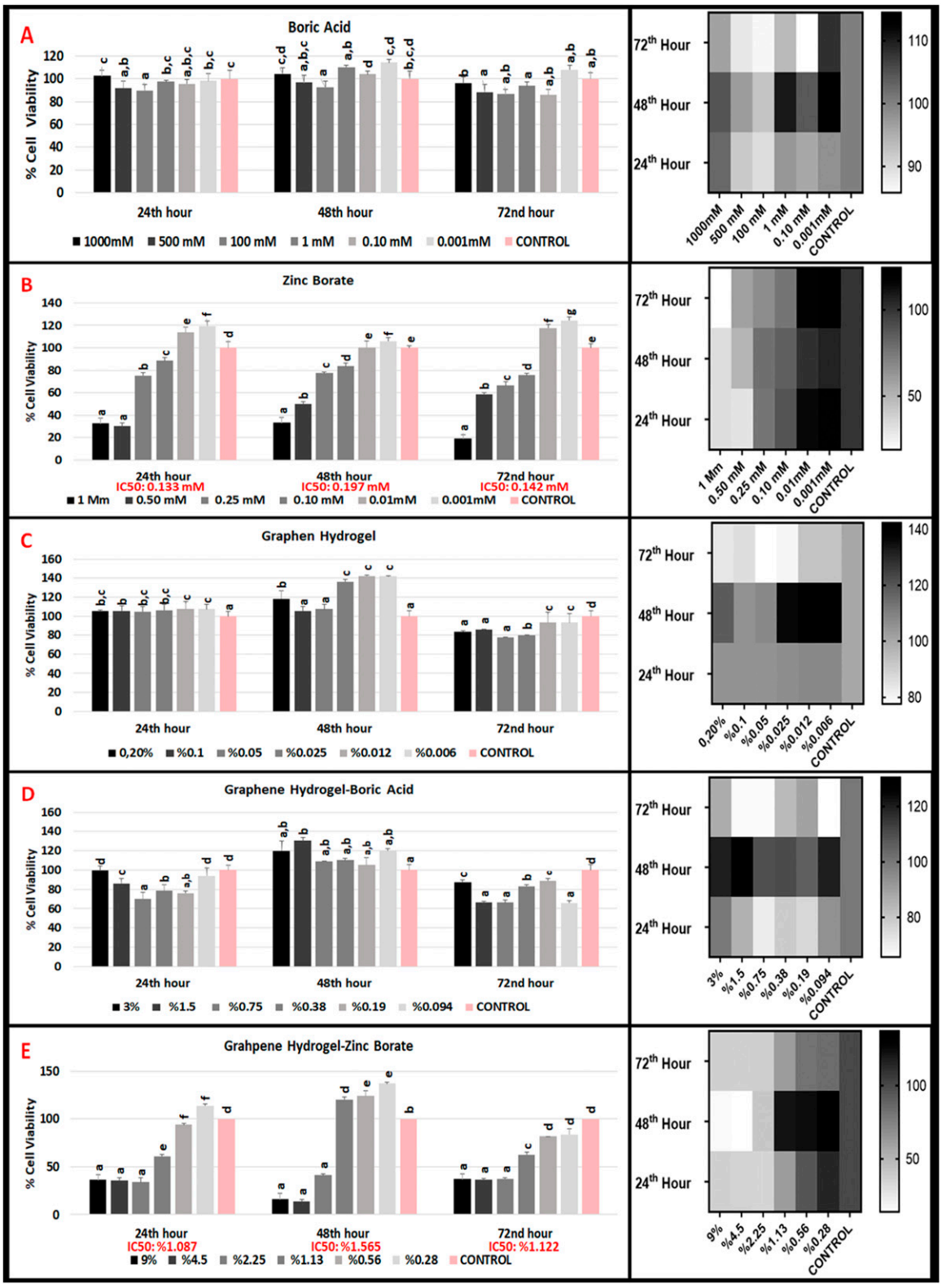


Figure 1. Effects of boric acid, zinc borate, graphene hydrogel, graphene hydrogel-boric acid and graphene hydrogel-zinc borate on L929 cell viability at 24th 48th and 72nd hours.

concentrations and it did not cause genotoxic damage.[34] From this perspective, our results are in harmony with literature.

Antioxidant Ability analyses of boron products. The proliferative effects of varying concentrations of boric acid (0.001 mM-1000 mM) and zinc borate (0.001 mM-1 mM) on the L929 (mouse fibroblast) cell line at 24, 48, and 72 h under H_2O_2 stress condition are shown in Figure 2. When the prophylactic effect of boric acid against oxidative stress induced by H_2O_2 (hydrogen peroxide) in L929 (mouse fibroblast) cells was compared with the control group at 24th, 48th and 72nd hours by applying 0.001 mM and 1000 mM concentrations, no significant proliferation or inhibition was observed in cells at any concentration (Figure 2(A)). The insignificant EC50 values and the statistical insignificance of the cell proliferation results from the concentration starting from 0.001 mM to 10000 mM show that boric acid did not have any positive or negative effect on the oxidative stress induced on L929 (mouse fibroblast) cells at 24th, 48th and 72nd hours. L929 cells treated with different concentrations of boric acid did not show a significant change in viability against the oxidative stress induced by H_2O_2.

When the prophylactic effect of zinc borate concentrations between 0.001 mM and 1 mM against the oxidative stress induced by H_2O_2 in L929 cells at the 24th, 48th and 72nd hours was compared with the control group, an increased prophylactic effect was observed with dose reduction (Figure 2(B)). The EC50 dose, which increased the proliferative concentration by 50%, at the 24th hour in cell proliferation was 0.051 mM, the EC50 dose at the 48th hour was 0.015 mM and the EC50 dose at the 72nd hour was 0.011 mM. In another words, Zinc borate has a proliferative effect on L929 cells from 0.001 mM to 0.051 mM, but has no prophylactic effect at concentrations higher than 0.051 mM at 24th hour. At 48th hour, it has proliferative effect between 0.001mM and 0.015 mM and at 72nd hour between 0.001mM and 0.011 mM. In higher concentrations, there is no prophylactic effects for 48th and 72nd hours. Our results for oxidative stress induced by H_2O_2 (hydrogen peroxide) in L929 (mouse fibroblast) cells has the same perspective with our cell viability results in boric acid and zinc borate. Looking at the literature, it has been observed that boric acid has a protective effect against free radical damage in many pathological conditions.[35,36] In zinc borate, no protective effect was observed against H_2O_2 at the first five concentrations, but it was found to have a protective effect against H_2O_2 at the last low concentrations. We think that this harmony is related to the antioxidant effect of BA and WB. Our results also show parallelism with the results of the studies conducted by Türkez et al., Üstündağ et al., Sarıkaya et al. in the literature.[37–39]

Cell migration test of boron products. A standard in vitro method, the Migration test (wound healing test), was performed to investigate the effect of boric acid and zinc borate on the migration of L929 cells into the scratch-induced wound area. 15 boric acid concentrations (1000 mM, 750 mM, 500 mM, 250 mM, 100 mM, 50 mM, 1 mM, 0.75 mM, 0.50 mM, 0.25 mM, 0.10 mM, 0.05 mM, 0.025 mM, 0.01 mM, 0.001 mM and five zinc borate 0.10 mM, 0.05 mM, 0.025 mM, 0.01 mM, 0.001 mM concentration was used in cell migration test. The microscopic images of 100 mM BA and 0.025 mM ZB, which give the best images, at 0, 12, and 24 h are shown in Figure 3(C). As in Figure 3(C), the area was calculated by calculating the aperture length, and the recovery rate at the 0th hour was assumed to be zero percent, and the improvements in all concentrations at the 24th hour were given in percent (%) Figure 3(A)–(B). In migration tests, the 24th hour is considered as the reference and the change is calculated according to the 0 hour. The results obtained are compared with the control group.[40] Accordingly, the migration recovery percentages of 15 concentrations of BA at 24 h were 62.46%, 81.62%, 70.05%, 75.56%, 87.11%, 87.55%, 73.18%, 83.24%, 80.92%, 86.54%, 77.98%, 83.57%, 81.05%, 70.81%, 86.91% respectively; the control group was found to be 62.84%. The closure percentages in the zinc borate concentrations used are between 75 and 90 %. Among the results of BA between 1000 mM and 0.75 mM, the best closure result compared to the control group was 87.11%. With the concentration 100 mM. The best closure result of zinc borate between 0.1 mM and 0.001 mM compared to the control group was 88.13% with 0.025 mM dose.

The similarity to the dose-independent fluctuating results seen in cell viability rates of BA was also revealed in the migration test. This may be due to the broad-spectrum antimicrobial properties of boric acid, which were also determined in our microbiology study, and its positive effect on cells responsible for wound healing. The very strong antioxidant properties of boric acid were reported by Yılmaz et al.[29] Therefore, boric acid may have shown a protective effect even at low doses. The results of our study are also in agreement with the clinical trials of boric acid by Kapukaya et al.[41] A similar result to the MTT test was also found in the ZB groups. The best healing rate was found to be around 88.5% in ZB6 (0.05 mM) and ZB7 (0.025 mM). The reason for the increase in migration compared to the control groups may be due to the antioxidant effect of ZB at non-cytotoxic doses.[42]

Analyses of boric acid and zinc borate doped graphene hydrogel products

Graphene hydrogel characterization. The resulting cylindrical graphene aerogels were 1.3 cm wide and 2.8 cm height.

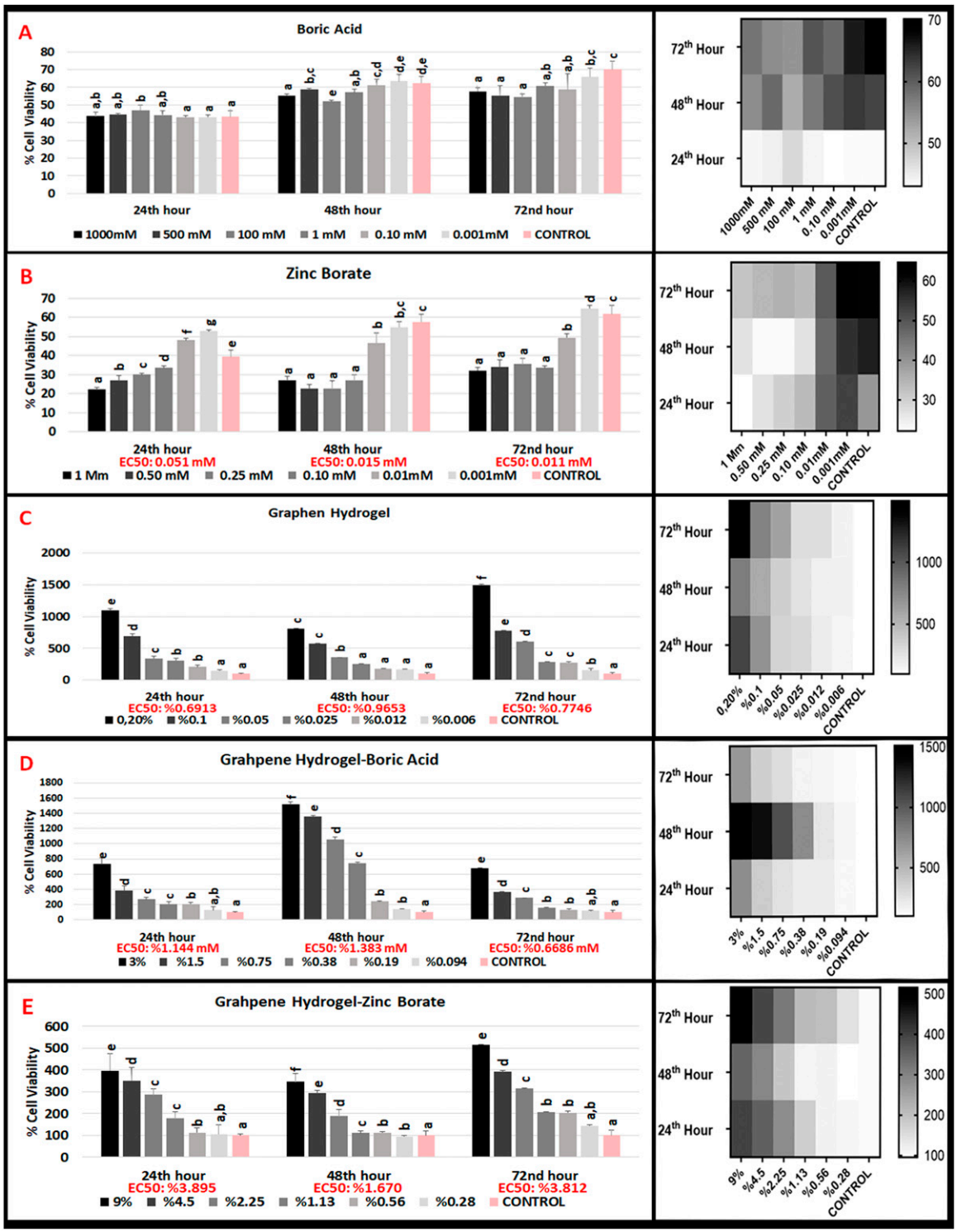


Figure 2. Effects of boric acid, zinc borate, graphene hydrogel, graphene hydrogel-boric acid and graphene hydrogel-zinc borate on L929 cell viability at 24th 48th and 72nd under H_2O_2 oxidative stress.

Then, different weight ratios of boric acid and zinc borate were added to graphene aerogels by liquid phase impregnation method. The morphology of blank graphene aerogel and boric acid and zinc borate doped graphene aerogels were examined by scanning electron microscope (SEM) and transmission electron microscope (TEM). SEM images of the prepared materials are shown in Figure 4. In Figure 4(a), it is seen that the graphene aerogels synthesized starting

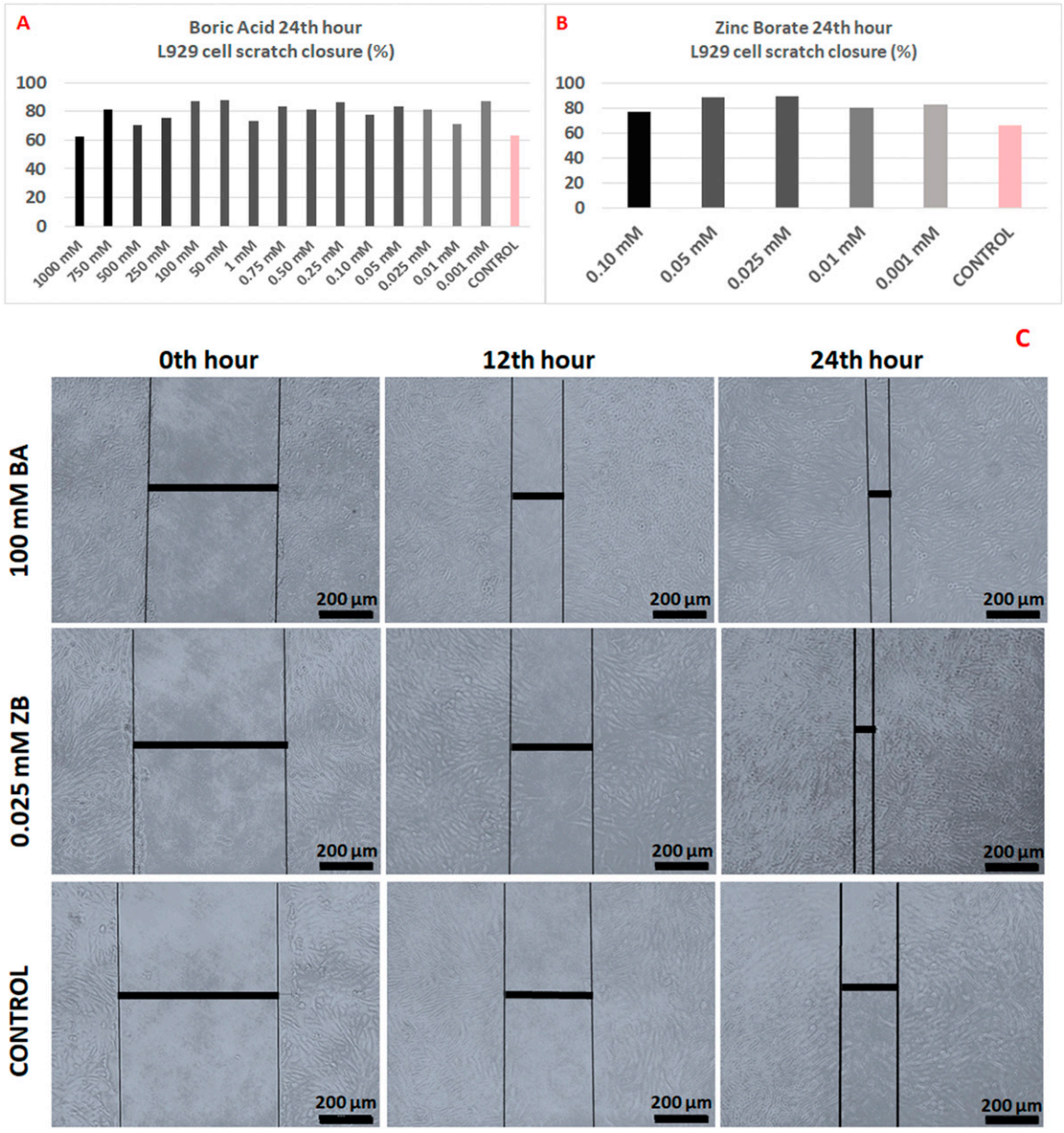


Figure 3. Boric acid and zinc borate cell closure percentages and migration images.

from graphene oxide have a reticulated structure with finely twisted graphene sheets and mesopores. In Figure 4(b), it is seen that the porous structure of the graphene aerogels disappeared after the boric acid doping, but the mesh-like structure was preserved, and the boric acid crystals were successfully doped between the thin sheets of the graphene aerogel. However, it is seen that the doped boric acid crystals are in micron size with irregular shapes. On the other hand, in Figure 4(c), it is understood that as a result of zinc borate doping, the initial structure of the graphene aerogel was preserved except for the pores, and the zinc borate crystals were successfully integrated into the graphene aerogel structure. It is clearly seen that the doped zinc borate crystals are in micron size like the boric acid crystals.

The TEM images of blank graphene aerogel, boric acid and zinc borate doped graphene aerogels are shown in Figure 4(g)–(i). A representative of TEM image of blank graphene aerogels shows that they composed of bended graphene nanosheets, the translucent nature of the bended nanosheets indicates that the nanosheets are relatively thin and thus the number of graphene layers is small. The space between these bended graphene nanosheets forms micrometer channels, which results in the microporous

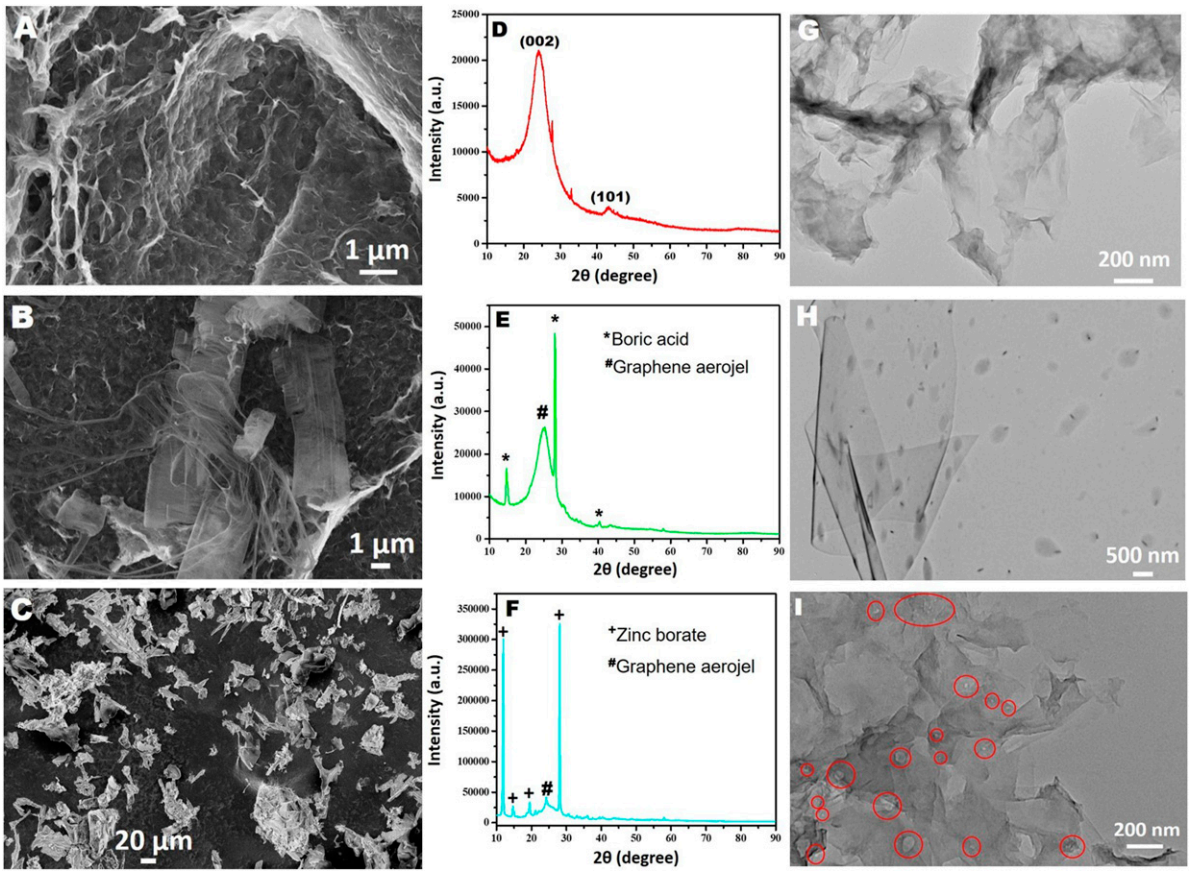


Figure 4. SEM images (A, B, and C), XRD patterns (D, E, and F), and TEM images (G, H, and i) of blank graphene aerogel, graphene aerogel doped with 1.5% by weight boric acid, and graphene aerogels doped with 4.5% by weight zinc borate, respectively.. (In Figure 4(i); the particles circled in red are zinc borate crystals).

structure and ultralight weight of graphene aerogels. Boric acid doping is clearly evident from the TEM image presented in Figure 4(h). Boric acid crystals are uniformly dispersed between the thin flake layers of the graphene aerogel. Particle size of boric acid crystals varies in the range of 0.5-2 µm. A TEM image of zinc borate loaded graphene aerogels (Figure 4(i)) shows that the zinc borate crystals are more evenly dispersed among the finely bended graphene nanosheets and have much smaller particle sizes than the boric acid crystals (the particles circled in red are zinc borate crystals).

After examining the morphologies of the prepared materials by SEM and TEM, their crystal structures were analyzed by powder X-ray diffraction (XRD). In Figure 4(d), XRD patterns of blank graphene aerogel, boron-doped and zinc-doped aerogels are presented. The two peaks observed at $2\theta = 24.5°$ and 44.5° in the XRD pattern of the graphene aerogel (Figure 4(d)) belong to the (002) and (100) planes of the graphene structure. The presence of these peaks indicates that the graphene oxide is reduced and the distance between the layers becomes smaller and a reticulated graphene aerogel structure is formed. On the other hand, when the XRD pattern of boric acid doped graphene aerogel is examined, two intense sharp peaks are observed at $2\theta = 15°$ and 28°, attributing the boric acid crystals (Figure 4(e)). In addition to these peaks of boric acid crystals, the (002) peak of graphene aerogel is also seen at $2\theta = 24.5°$. Finally, the peaks observed at $2\theta = 11°$, 14°, 19° and 28° in the XRD pattern of the zinc borate doped graphene aerogel clearly indicate the presence of zinc borate crystals in the structure (Figure 4(f)).

X-ray photoelectron spectroscopy (XPS) is one of the most effective methods for the analysis of the chemical composition of material surfaces. In this context, XPS analysis of blank graphene aerogel, boric acid and zinc borate doped graphene aerogels were. The XPS survey spectra of three materials are shown in Figure 5(a), (c), and (e). Upon the comparison of the XPS spectra of the three materials, it can be concluded that boric acid and zinc borate are successfully doped into graphene aerogels. On the other hand, from the high resolution C1s XPS spectrum of the empty graphene aerogel, it is seen that there are three different bonds of C atoms (C-C, C-O-C and O-C = O) in the graphene aerogel structure, and this result is compatible

with the literature. The expected B-B, B-O and B-H bonds are observed in the high resolution B 1s XPS spectrum of the boron doped graphene aerogel. Finally, in the high resolution Zn 2p XPS spectrum of the zinc borate doped graphene aerogel, it is understood that the zinc atoms are in the +2 oxidation state and there is no change in the zinc borate structure as a result of the doping.

Although there are many graphene aerogel synthesis reported in the literature, zinc borate and boric acid doped graphene aerogel synthesis has not been reported yet.[43] In

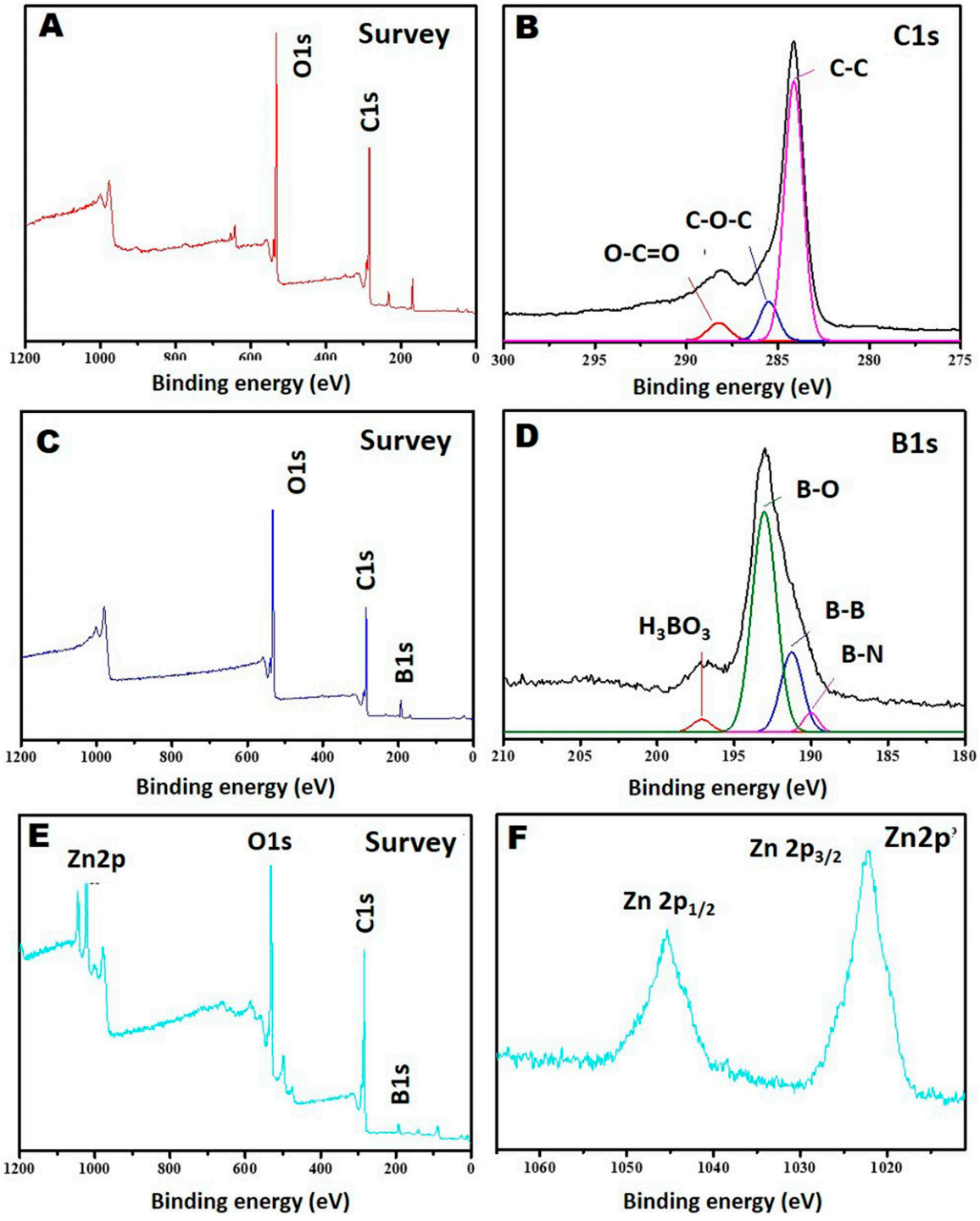


Figure 5. XPS spectra of a, (b) blank graphene aerogel, c, (d) 1.5% by weight boric acid doped graphene aerogel and e, (f) 3% weight zinc borate doped graphene aerogels.

this study, zinc borate and boric acid doped superlight graphene aerogels were synthesized and their biocompatibility was proven for the first time.

Biological characterization analyses of boric acid and zinc borate doped graphene hydrogel. Cell viability and hydrogen peroxide (H_2O_2) induced oxidative stress tests were performed by sterilizing the products in concentrations of 0.006%–0.20% for empty GH, 0.094% −3 % for BA doped graphene hydrogels, and 0.28% −9 % for WB doped graphene hydrogels (6 different concentrations per analyses).

Cytotoxicity analyses of boron products doped graphene hydrogel. When the effects of six different concentrations (0.2%-0.006%) of pure graphene hydrogels on L929 (mouse fibroblast) cells at 24th hour were compared with the control group, concentration between (0.20-0.025 %) showed no statistical difference in terms of cell viability (Figure 1(C)). Low concentrations (0.012% and 0.006%) of pure graphene hydrogels has a statistically significant increase in cell viability. At 48th hour, there is a significant difference in 0.025, 0.012 and 0.006 concentration (low concentration) of pure graphene hydrogels when compared to control group for cell viability. At 72nd hour, all concentrations of pure graphene hydrogels have a significant difference versus control group. The IC50 dose of the inhibitor concentration, which caused a 50% reduction in cell proliferation, could not be determined for all times we measured for pure graphene hydrogels.

When the effect of boric acid doped graphene hydrogels (0.094% - 3%) (Figure 1(D)) on L929 (mouse fibroblast) cells at 24 h was evaluated, the groups at all concentrations (3% - 0.094%) were statistically significant, except the lowest and highest dose, versus the control group. At the 48th hour, there was no statistically significant difference when all concentrations of boric acid doped graphene hydrogels were compared with the control group, except for the 1.5% group. At 72 h, all concentrations were statistically significant when compared with the control group. The IC50 dose of the inhibitor concentration could not be determined for all times we measured for boric acid doped graphene hydrogels

When the effect of Graphene hydrogel-zinc borate (0.028% - 9%) groups (Figure 1(E)) on L929 cells at 24th hour was compared with the control group, there was a statistically significant difference. An inhibitory effect was observed at higher concentrations (9%–0.56%) compared to control. The IC50 dose was found to be 1.087%. At 48th hour, a statistically significant difference was observed at all concentrations (except 1.13% and 0.56%) when compared with the control group. While there was an inhibitory effect at high doses (9%–2.25%) compared to the control, a proliferative effect was observed in the 0.28% group. The IC50 dose was found to be 1.565%. At 72nd hour, a significant difference was observed compared to the control at all concentrations. The IC50 dose was 1.12%.

Antioxidant Ability analyses of boron products doped graphene hydrogel. Evaluating the effect of H_2O_2 oxidative stress test on L929 cells in Graphene hydrogel groups at 24th hour (Figure 2(C)), all concentrations were statistically significant versus control, except for the GH 0.006% group. An increase in proliferation was observed with an increase in concentration in GH groups. Protection against cellular oxidative damage was obtained with increasing concentration in all groups except 0.006% group. All concentrations of Graphene hydrogel at 48th hour were statistically significant relative to the control, except the 0.006%–0.025% groups. Protection against cellular oxidative damage increased with increasing concentration in all groups. When all GH groups are evaluated among themselves, an increase in proliferation and an increase in protective effect against oxidative damage are observed with an increase in concentration (except 0.006% and 0.012%). At 72nd hour, there was a significant difference at all concentrations. There was a correlation between dose increase and protection against cellular oxidative damage. An increase in proliferation is observed with increasing doses of GH groups.

All concentrations of boric acid doped Graphene hydrogel were significantly different compared to the control group when the protective effect was evaluated in the 24th hour H_2O_2 oxidative stress test (Figure 2(D)). Protection against cellular oxidative damage increased with increasing concentration at all concentrations except the 0.094% group. An increase in proliferation was observed with increasing dose at 0.19% concentration and higher G-BA concentrations. All G-BA concentrations at 48th and 72nd hours are significant relative to control. Protection against cellular oxidative damage was obtained with increasing concentration at all concentrations. In the G-BA groups, the increase in the dose and the increase in proliferation were parallel.

All concentrations of zinc borate doped Graphene hydrogel were significantly different compared to the control group when the protective effect was evaluated in the 24th hour H_2O_2 oxidative stress test (Figure 2(E)). Protection against cellular oxidative damage increased with increasing concentration at all concentrations. An increase in proliferation was observed with increasing concentration at all G-ZB groups. All G-ZB concentrations, except 0.28%, at 48th and 72nd hours are significant relative to control. Protection against cellular oxidative damage was obtained with increasing concentration at all concentrations. A correlational protection against cellular oxidative damage was obtained with increasing concentration in all groups. In all G-ZB groups, the increase in the dose and the increase in proliferation were parallel.

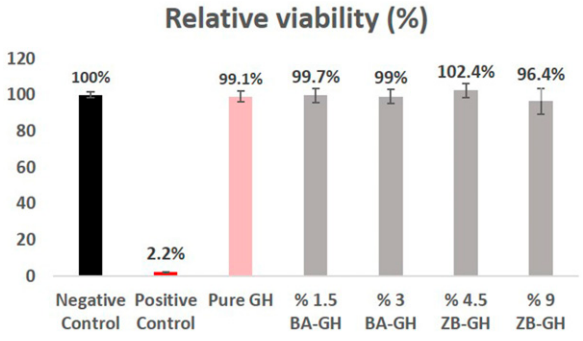


Figure 6. The relative cell viability (%) after exposure of graphene hydrogel in Epiderm SIT in vitro irritation test.

In Vitro EpiDerm™ Skin Irritation Test of Boric Acid and Zinc borate doped Graphene Hydrogel

According to the testing results none of the graphene hydrogel that tested did not induce skin irritation since the mean relative viability was not reduce below 50% of the mean viability of NCs due to exposure of hydrogels. Positive control (5% SDS) were also in accepted range (relative viability below %20) criterion according to the manufacturer's protocol. Consequently, it might be suggested that both graphene hydrogel did not induce dermal irritation and it can be safely used for wound healing Figure 6.

Results represent the mean + SD of three individual tissues. NC: negative control (DPBS); PC: positive control (5% SDS); 1: Blank graphene hydrogel; 2: 1.5% boric acid containing graphene hydrogel; 3: 3% boric acid containing graphene hydrogel; 4: 4.5% zinc borate containing graphene hydrogel; 5: 9% % zinc borate containing graphene hydrogel

Irritation potential of graphene hydrogels was evaluated with the validated alternative in vitro EpiDerm SIT in this study. All the tested graphene hydrogels were nonirritant according to the European Union (EU) and Globally Harmonized System (GHS) classification because chemicals are classified as nonirritant if the treated tissue viability relative to the negative control is reduced below 50%. This test is validated for in vitro skin irritation testing of chemicals, including cosmetic and pharmaceutical ingredient.[25] In our study hydrogels synthesized for the wound healing and they should be biocompatible without affecting the biological and physical nature of the dermal tissues. The EpiDerm SIT test results showed us that the developed product for the wound healing can be used for application in biomedical and daily therapy for wounds with no harmful effects in terms of dermal irritation with a potent antimicrobial activity. In the literature, there are different biomedical device based on hydrogels were developed for different application areas in human health.[44–46] The increasing use of these materials has raised questions about their efficacy and safety and good biocompability is an important point in developing. In Liang Y et al study the Adhesive Hemostatic Conducting Injectable Composite Hydrogels were developed for wound healing therapy. L929 cell were used for the evaluation and confirmed the biocompability of these materials.[46] In another study in vivo test performed with the New Zealand white rabbits for the skin irritation study for the lidocaine-loaded reduced graphene oxide hydrogel and this graphene oxide based topical hydrogel found to be safe because of no sign of irritation in rabbit's application area.[45] Graphene-based materials evaluated by Fusco et al for their skin irritation potential with the experiments was carried out following OECD TG 439, using the SkinEthic™ Skin Irritation Test-42bis (42 min exposure +42 h post-incubation). While few-layer graphene (FLG), graphene oxide (GO), reduced GO and CVD-graphene are classified as non-irritant, FLG exfoliated with sodium dodecyl sulfate or sodium dodecylbenzenesulfonate were found to be irritant for the skin.[44] When evaluated all the study in general graphene based materials are non-irritant as we found in our study but some different developing methods of these materials leads can be increased irritation potential of these materials probably because of the different developing steps or used materials.

Conclusions

As a result, it has been shown that the investigated substances Boric acid, zinc borate, graphene hydrogel, graphene-boric acid and graphene-zinc borate are non-toxic in the determined concentration range, can resist oxidant damage and increase cell migration. The antimicrobial properties of boric acid and zinc borate even at very low concentrations contributed to the emergence of these effects. In this study, zinc borate and boric acid doped superlight graphene hydrogels were synthesized and characterized for the first time in the literature, and their biocompatibility was proved for the first time.

Acknowledgments

We would like to express our special thanks to The Scientific and Technological Research Council of Turkey (TÜBİTAK) to support us with the grand number 119S510.

Declaration of conflicting interests

The author(s) declared no potential conflicts of interest with respect to the research, authorship, and/or publication of this article.

Funding

The author(s) disclosed receipt of the following financial support for the research, authorship, and/or publication of this article: This study is supported by TÃ¼rkiye Bilimsel ve Teknolojik AraÅŸtÄ±rma Kurumu; 119S510.

ORCID iDs

Yasin Bayir https://orcid.org/0000-0003-3562-6727
Emir Enis Yurdgulu https://orcid.org/0000-0002-9636-1753

References

1. Murray FJ. A comparative review of the pharmacokinetics of boric acid in rodents and humans. *Biol Trace Elem Res* 1998; 66: 331–341.
2. Tepedelen BE, Soya E and Korkmaz M. Boric acid reduces the formation of DNA double strand breaks and accelerates wound healing process. *Biol Trace Elem Res* 2016; 174(2): 309–318. DOI: 10.1007/s12011-016-0729-9.
3. Abdelnour SA, Abd El-Hack ME, Swelum AA, et al. The vital roles of boron in animal health and production: a comprehensive review. *J Trace Elem Med Biol* 2018; 50: 296–304. DOI: 10.1016/j.jtemb.2018.07.018.
4. Hinz B. The role of myofibroblasts in wound healing. *Curr Res Transl Med* 2016; 64(4): 171–177. DOI: 10.1016/j.retram.2016.09.003.
5. Lindley LE, Stojadinovic O, Pastar I, et al. Biology and biomarkers for wound healing. *Plast Reconstr Surg* 2016; 138(3 Suppl): 18S–28S. DOI: 10.1097/PRS.0000000000002682.
6. Shaw TJ and Martin P. Wound repair at a glance. *J Cell Sci* 2009; 122(Pt 18): 3209–3213. DOI: 10.1242/jcs.031187.
7. Eming SA, Martin P and Tomic-Canic M. Wound repair and regeneration: mechanisms, signaling, and translation. *Sci Transl Med* 2014; 6(265): 265sr6. DOI: 10.1126/scitranslmed.3009337.
8. Borthwick LA, Wynn TA and Fisher AJ. Cytokine mediated tissue fibrosis. *Biochim Biophys Acta* 2013; 1832(7): 1049–1060. DOI: 10.1016/j.bbadis.2012.09.014.
9. Zhuang B, Chen T, Xiao Z, et al. Drug-loaded implantable surgical cavity-adaptive hydrogels for prevention of local tumor recurrence. *Int J Pharm* 2020; 577: 119048. DOI: 10.1016/j.ijpharm.2020.119048.
10. Stephen JB, Ding CZ, Akama T, Zhang Y-K, et al. Therapeutic potential of boron-containing compounds. *Future Med Chem*. 2009, October;1(7):1275-1288. doi: 10.4155/fmc.09.71.
11. Büyük B, Aydeğer C, Adalı Y, et al. The effect of topically applied boric acid on ephrin-eph pathway in wound treatment: an experimental study. *Int J Low Extrem Wounds* 2021;13: 15347346211055260. DOI: 10.1177/15347346211055260.
12. Chebassier N, Ouijja EH, Viegas I, et al. Stimulatory effect of boron and manganese salts on keratinocyte migration. *Acta Derm Venereol* 2004; 84(3): 191–194.
13. Demirci S, Dogan A, Aydin S, et al. Boron promotes streptozotocin-induced diabetic wound healing: roles in cell proliferation and migration, growth factor expression, and inflammation. *Mol Cell Biochem* 2016; 417(1-2): 119–133. DOI: 10.1007/s11010-016-2719-9.
14. Ege D, Nawaz Q, Beltran AM, et al. Effect of boron-doped mesoporous bioactive glass nanoparticles on C2C12 cell viability and differentiation: potential for muscle tissue application. *ACS Biomater Sci Eng* 2022; 8(12): 5273–5283. DOI: 10.1021/acsbiomaterials.2c00876.
15. Gupta M, Mahajan VK, Mehta KS, et al. Zinc therapy in dermatology: a review. *Dermatol Res Pract* 2014; 2014: 709152. DOI: 10.1155/2014/709152.
16. Baltaci AKMR, Mogulkoc R and Baltaci SB. Review: the role of zinc in the endocrine system. *Pak J Pharm Sci* 2019; 32(1): 231–239.
17. Kokabi M, Sirousazar M and Hassan ZM. PVA-clay nanocomposite hydrogels for wound dressing. *Eur Polym J* 2007; 43(3): 773–781. DOI: 10.1016/j.eurpolymj.2006.11.030.
18. Metin O, Kayhan E, Ozkar S, et al. Palladium nanoparticles supported on chemically derived graphene: an efficient and reusable catalyst for the dehydrogenation of ammonia borane. *Int J Hydrogen Energy* 2012; 37(10): 8161–8169. DOI: 10.1016/j.ijhydene.2012.02.128.
19. Ai KL, Liu YL, Lu LH, et al. A novel strategy for making soluble reduced graphene oxide sheets cheaply by adopting an endogenous reducing agent. *J Mater Chem* 2011; 21(10): 3365–3370. DOI: 10.1039/c0jm02865g.
20. Das S, Irin F, Ma L, et al. Rheology and morphology of pristine graphene/polyacrylamide gels. *Acs Appl Mater Inter* 2013; 5(17): 8633–8640. DOI: 10.1021/am402185r.
21. Clinical and Laboratory Standards Institute. *(CLSI): Performance standards for antimicrobial susceptibility testing. 24th informational supplement. Document M100-S24, CLSI*, Wayne, PA, USA: CLSI. 2014.
22. Clinical and Laboratory Standards Institute (CLSI). *Reference method for Broth dilution antifungal susceptbility testing of yeasts; 4th informational supplement, M27-S4*. Wayne PA, USA: CLSI. 2014.
23. Metin Ö, Ho SF, Alp C, et al. Ni/Pd core/shell nanoparticles supported on graphene as a highly active and reusable catalyst for Suzuki-Miyaura cross-coupling reaction. *Nano Res* 2013; 6(1): 10. DOI: 10.1007/s12274-012-0276-4.
24. OECD. Test No. 439: in vitro skin irritation: reconstructed human epidermis test method. In: *OECD guidelines for the testing of chemicals, section 4*. Paris: OECD Publishing, 2021.
25. Kandarova H, Willoughby JA, De Jong WH, et al. Prevalidation of an in vitro skin irritation test for medical devices using the reconstructed human tissue model EpiDerm. *Toxicol Vitro* 2018; 50: 407–417. DOI: 10.1016/j.tiv.2018.02.007.
26. Sayin Z, Ucan US and Sakmanoglu A. Antibacterial and antibiofilm effects of boron on different bacteria. *Biol Trace Elem Res* 2016; 173(1): 241–246. DOI: 10.1007/s12011-016-0637-z.
27. Ulu A, Balcioglu S, Birhanli E, et al. Poly(2-hydroxyethyl methacrylate)/boric acid composite hydrogel as soft contact lens material: thermal, optical, rheological, and enhanced antibacterial properties. *J Appl Polym Sci* 2018; 135(35): 46575. DOI: 10.1002/app.46575.
28. Rowe RI, Bouzan C, Nabili S, et al. The response of trout and zebrafish embryos to low and high boron concentrations is

U-shaped. *Biol Trace Elem Res* 1998; 66(1-3): 261–270. DOI: 10.1007/BF02783142.
29. Yılmaz S, Ustundag A, Cemiloglu Ulker O, et al. Protective effect of boric acid on oxidative DNA damage in Chinese hamster lung fibroblast V79 cell lines. *Cell J* 2016; 17(4): 748–754.
30. Bennett A, Rowe RI, Soch N, et al. Boron stimulates yeast (Saccharomyces cerevisiae) growth. *J Nutr* 1999; 129(12): 2236–2238.
31. Park M, Li Q, Shcheynikov N, et al. NaBC1 is a ubiquitous electrogenic Na+-coupled borate transporter essential for cellular boron homeostasis and cell growth and proliferation. *Mol Cell*. 2004;16(3):331-341. Doi: 10.1016/j.molcel.2004.09.030.
32. Devirian TA and Volpe SL. The physiological effects of dietary boron. *Crit Rev Food Sci*. 2003;43(2):219-231. Doi: 10.1080/10408690390826491.
33. Pawa S and Ali S. Boron ameliorates fulminant hepatic failure by counteracting the changes associated with the oxidative stress. *Chem Biol Interact* 2006; 160(2): 89–98. DOI: 10.1016/j.cbi.2005.12.002.
34. ÇelikezenTürkezToğar FÇHB and Toğar B. In vitro assessment of genotoxic and oxidative effects of zinc borate. *Toxicol Environ Chem* 2014; 96(5): 777–782.
35. Barranco WT and Eckhert CD. Cellular changes in boric acid-treated DU-145 prostate cancer cells. *Br J Cancer* 2006; 94(6): 884–890. DOI: 10.1038/sj.bjc.6603009.
36. Geyikoglu F and Turkez H. Boron compounds reduce vanadium tetraoxide genotoxicity in human lymphocytes. *Environ Toxicol Pharmacol* 2008; 26(3): 342–347. DOI: 10.1016/j.etap.2008.07.002.
37. Sarikaya R, Erciyas K, Kara MI, et al. Evaluation of genotoxic and antigenotoxic effects of boron by the somatic mutation and recombination test (SMART) on Drosophila. *Drug Chem Toxicol* 2016; 39(4): 400–406. DOI: 10.3109/01480545.2015.1130719.
38. Turkez H, Tatar A, Hacimuftuoglu A, et al. Boric acid as a protector against paclitaxel genotoxicity. *Acta Biochim Pol* 2010; 57(1): 95–97.
39. Ustundag A, Behm C, Follmann W, et al. Protective effect of boric acid on lead- and cadmium-induced genotoxicity in V79 cells. *Arch Toxicol* 2014; 88(6): 1281–1289. DOI: 10.1007/s00204-014-1235-5.
40. Santos JAA, da Silva JW, dos Santos SM, et al. In vitro and in vivo wound healing and anti-inflammatory activities of babassu oil (attalea speciosa mart. Ex spreng., arecaceae). *Evid-based Complement Altern Med* 2020; 2020: 8858291. DOI: 10.1155/2020/8858291.
41. Kapukaya R and Ciloglu O. Treatment of chronic wounds with polyurethane sponges impregnated with boric acid particles: a randomised controlled trial. *Int Wound J* 2020; 17(5): 1159–1165. DOI: 10.1111/iwj.13463.
42. Aysel U, Ceylan O, Boran R, et al. A new approach for prevention the oxidations and mutations: zinc borate. *Bor Dergisi* 2019; 4(4): 196–202.
43. Fu Y, Wang G, Mei T, et al. Accessible graphene aerogel for efficiently harvesting solar energy. *ACS Sustainable Chem Eng* 2017; 5(6): 4665–4671. DOI: 10.1021/acssuschemeng.6b03207.
44. Fusco L, Garrido M, Martin C, et al. Skin irritation potential of graphene-based materials using a non-animal test. *Nanoscale* 2020; 12(2): 610–622. DOI: 10.1039/c9nr06815e.
45. Li W, Zhang G and Wei X. Lidocaine-loaded reduced graphene oxide hydrogel for prolongation of effects of local anesthesia: in vitro and in vivo analyses. *J Biomater Appl* 2021; 35(8): 1034–1042. DOI: 10.1177/0885328220988462.
46. Liang Y, Zhao X, Hu T, et al. Adhesive hemostatic conducting injectable composite hydrogels with sustained drug release and photothermal antibacterial activity to promote full-thickness skin regeneration during wound healing. *Small* 2019; 15(12): e1900046. DOI: 10.1002/smll.201900046.